

the weighted average of γ_M and γ_S (25). Therefore,

$$\gamma_f = f\gamma_S + (1 - f)\gamma_M \quad (2)$$

The resulting interfacial energies γ_{Sf} and γ_{Mf} and the interfacial energy difference $\Delta\gamma(f) = \gamma_{Mf} - \gamma_{Sf}$ are shown in Fig. 3, A and B. $\gamma_{Mf} = \gamma_{Sf}$ at $f = 0.57 \pm 0.05$. The uncertainty in f results from uncertainties in the contact angles. When $\gamma_{Sf} = \gamma_{Mf}$, the interactions between the polymers and the surface are balanced and the surface is neutral. Thus, grafting a random copolymer brush with this composition onto a surface will produce a surface with no preferential affinity for either component.

Because the homopolymer penetrates several nanometers into the random copolymer brush, these experiments do not provide information on the composition of the random copolymer immediately at the surface. X-ray photoelectron spectroscopy cannot provide quantitative information, because MMA portions of the random copolymer can decompose in the x-ray beam. To address this, the contact angle of water (θ_w) on the random copolymer brush surfaces was measured as a function of f (Fig. 4). θ_w increased monotonically with the styrene content of the copolymer, possibly saturating at higher values of f . These results show that the surface energy can be tuned precisely between that of PS and PMMA, and that the composition of the brush at the surface is quite similar to that in the interior of the brush.

By simply varying the composition of a random copolymer grafted onto a surface, the wetting behavior of a homopolymer on that surface can be changed in a highly controllable fashion. This technique should prove especially useful for controlling the surface behavior of polymer blends and block copolymers, because the relative surface affinity of the two components can be precisely controlled. Thus, it is a simple matter to produce a surface having non-preferential interactions for a given pair of polymers. This method is applicable to any pair of polymers for which an end-functionalized random copolymer can be prepared in a well-controlled fashion. Other architectures besides linear copolymerization may also be used, such as graft copolymers with controllable graft length and density. The method discussed here should also be useful in controlling the interfacial behavior of simple fluids and in modifying surfaces to achieve biocompatibility.

REFERENCES AND NOTES

1. J. W. Cahn, *J. Chem. Phys.* **66**, 3667 (1977).
2. M. R. Moldover and J. W. Cahn, *Science* **207**, 1073 (1980).
3. P. Wiltzius and A. Cumming, *Phys. Rev. Lett.* **66**,

- 3000 (1991).
4. R. A. L. Jones *et al.*, *ibid.*, p. 1326.
5. W. Zhao *et al.*, *Macromolecules* **24**, 5991 (1991).
6. L. J. Norton *et al.*, *ibid.* **28**, 8621 (1995).
7. C. S. Henke, E. L. Thomas, L. J. Fetters, *J. Mat. Sci.* **23**, 1685 (1988).
8. G. Coulon, V. R. Deline, P. F. Green, T. P. Russell, *Macromolecules* **22**, 2581 (1989).
9. S. H. Anastasiadis, T. P. Russell, S. K. Satija, C. F. Majkrzak, *Phys. Rev. Lett.* **62**, 1852 (1989).
10. C. Nojiri *et al.*, *J. Biomed. Res.* **24**, 1151 (1990).
11. C. D. Bain, H. A. Biebuyck, G. M. Whitesides, *Langmuir* **5**, 723 (1989).
12. D. G. Walton *et al.*, *Macromolecules* **27**, 6225 (1994).
13. G. J. Kellogg *et al.*, *Phys. Rev. Lett.* **76**, 2503 (1996).
14. M. K. Georges, R. P. N. Veregin, P. M. Kazmaier, G. K. Hamer, *Macromolecules* **26**, 2987 (1993).
15. I. Li *et al.*, *ibid.* **28**, 6692 (1995).
16. C. J. Hawker, *J. Am. Chem. Soc.* **116**, 11185 (1994).
17. _____ *et al.*, *Macromolecules* **29**, 2686 (1996).
18. S. H. Anastasiadis *et al.*, *J. Chem. Phys.* **92**, 5677 (1990).
19. G. Reiter, P. Auroy, L. Auvray, *Macromolecules* **29**, 2150 (1996).
20. Films prepared from nonfunctionalized PS and

PMMA homopolymers could be completely removed from the surface by rinsing with toluene. The grafted layers, on the other hand, could be immersed in toluene at 50° to 60°C for several hours without changing the thickness of the grafted layer after drying.

21. L. Leibler *et al.*, in *Ordering in Macromolecular Systems*, A. Teramoto, M. Kobayashi, T. Norisue, Eds. (Springer-Verlag, Berlin, 1994), p. 301.
22. E. Vitt and K. R. Shull, *Macromolecules* **28**, 6349 (1995).
23. T. Young, *Philos. Trans.* **95**, 69 (1805).
24. S. Wu, *Polymer Interfaces and Adhesion* (Marcel Dekker, New York, 1982).
25. D. Urban, K. Topolski, J. DeConnick, *Phys. Rev. Lett.* **76**, 4388 (1996).
26. S. T. Milner and G. H. Fredrickson, *Macromolecules* **28**, 7953 (1995).
27. This work was partially supported by the U. S. Department of Energy's Office of Basic Energy Sciences, the NSF Center for Polymer Interfaces and Macromolecular Assemblies (Stanford/IBM/UC Davis), and the Materials Research Science and Engineering Center at the University of Massachusetts.

4 November 1996; accepted 21 January 1997

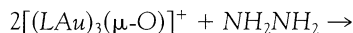
Dinitrogen Bridged Gold Clusters

Hui Shan, Yi Yang, Alan J. James, Paul R. Sharp*

A family of dinitrogen complexes, $[(LAu)_6(N_2)]^{2+}$ (L = a phosphine), with the dinitrogen unit bridging two clusters of three gold atoms have been prepared from hydrazine and $[(LAu)_3(O)]^+$. Structural characterization of the PPh_2^iPr (Ph, phenyl; iPr , isopropyl) derivative shows a nitrogen-nitrogen single-bond distance indicative of hydrazido (N_2^{4-}) character for the dinitrogen unit. The complexes can be reduced and protonated to give low [13% when L = PPh_2Me (Me, methyl)] to quantitative [100% when L = $P(p-MeOC_6H_5)_3$] yields of ammonia, establishing that bonding of dinitrogen to six metal atoms can lead to facile cleavage of the nitrogen-nitrogen bond.

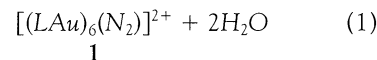
Many metal- N_2 complexes are known, the vast majority of which involve only one or two metal atoms, with just a few involving three metal atoms (Fig. 1) (1). Here, we report the preparation and characterization of a family of N_2 complexes with six metal atoms, in clusters of three, bonding simultaneously to the N_2 unit. In addition, these N_2 complexes can be reduced and protonated to give NH_3 , establishing that N_2 in such an environment can be activated, leading to reduction to NH_3 .

The synthesis of the N_2 complexes— $[(LAu)_6(N_2)]^{2+}$ (1) with L = PPh_2Me , PPh_2Et (Et, ethyl), PPh_3 (2), $P(p-MeOC_6H_5)_3$, $P(p-MeOC_6H_5)_3$, $P(p-CF_3C_6H_5)_3$, PPh_2^iPr , or $P(o-MeC_6H_5)_3$ —involves the addition of excess (2 to 3 equivalents) anhydrous hydrazine to dichloromethane solutions of $[(LAu)_3(\mu-O)]^+$ (3) as BF_4^- , PF_6^- , or $CF_3SO_3^-$ salts



Department of Chemistry, University of Missouri, Columbia, MO 65211, USA.

*To whom correspondence should be addressed. E-mail: chempr@showme.missouri.edu



The addition of diethylether or pentane to the reaction mixtures gives the products as thermally stable yellow to orange-yellow solids in 80 to 98% yield based on Au. The complexes were characterized by elemental analyses and nuclear magnetic resonance spectroscopy (4). We determined the structure of three derivatives by single-crystal x-ray diffraction analyses. Two of these are salts of 1 with L = PPh_3 and showed apparent multiple phenyl ring and anion orientations. The orientational disorder could not be adequately modeled, and the structure of a third derivative was determined. The structure of 1 with L = PPh_2^iPr , as the BF_4^- salt, is well ordered (5) (Fig. 2). The dication 1 in this structure is situated on an inversion center, and the overall core structure is that of a trigonally elongated octahedron (a trigonal antiprism) of Au atoms with the N_2 lying at the center along the trigonal axis. The same core structure is observed in the disordered structures of 1 with L = PPh_3 .

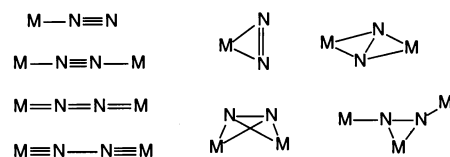


Fig. 1. Bonding modes for N_2 in metal complexes. M = a metal atom with associated ligands.

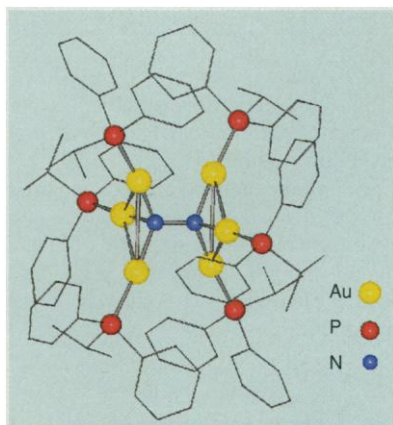


Fig. 2. The x-ray structure of the dication **1** (L = PPh_2Pr) in crystals of the BF_4^- salt. The anions are not shown, hydrogen atoms are omitted for clarity, and carbon atoms are drawn as points. Selected bond distances (in angstroms) and angles (in degrees): Au-P: 2.253(2), 2.238(3), 2.253(2); Au-N: 2.047(8), 2.047(7), 2.043(7); Au-Au: 3.2332(5), 3.3202(5), 3.1802(5); N-N: 1.475(14); Au-N-Au: 104.3(3), 108.5(3), 102.1(3); Au-N-N: 114.7(6), 110.3(7), 115.5(7).

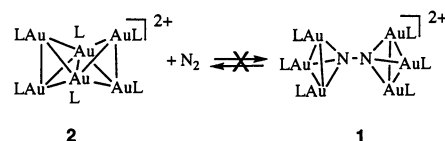


Fig. 3. A large kinetic barrier separating **1** from **2** + N_2 is suggested by the thermal stability of **1** and the absence of a reaction between **2** and N_2 .

The N-N distance in **1** of 1.475(14) Å (the numbers in parentheses being the standard error in the last digits) is typical of a N-N single bond such as is found in hydrazine (1.45 Å) (6). This N-N distance is the longest observed in a N_2 complex and indicates hydrazido (N_2^{4-}) character for the N_2 ligand. Distances previously observed in N_2 complexes considered to have hydrazido character fall in the range 1.25 to 1.34 Å. An average Au-N distance of 2.046 Å is found for **1**. The Au-Au distances of 3.2332(5), 3.3202(5), and 3.1802(5) Å within each triangular cluster of Au atoms are typical of "aurophilic" Au(I)-Au(I) bonds, which fall between 3.0 and 3.4 Å in length (7). Aurophilic bonds have been attributed to relativistic effects on the valence electrons of Au (8) and, with energies on the order of hydrogen bonds (7, 9), help

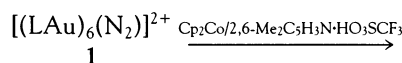
Table 1. Ammonia and hydrazine yields from $[(LAu)_6(N_2)]^{2+}$ **1** (estimated error, 5%). Cone angle is a measure of the phosphine steric bulk (14), and pK_a , where K_a is the acid constant, is a measure of the phosphine basicity (15).

Phosphine (L)	NH_3 yield (%)	Hydrazine yield (%)	pK_a	Cone angle
PPh_2Me	13	75	4.57	136
PPh_2Et	35	65	4.9	140
$P(p-CF_3C_6H_4)_3$	97	2	1.0*	145
PPh_3	54	46	2.73	145
$P(p-MeC_6H_4)_3$	94	5	3.84	145
$P(p-MeOC_6H_4)_3$	100	0	4.59	145
PPh_2Pr	80	20	5.0†	150
$P(o-MeC_6H_4)_3$	70	30	3.08	194

*Estimate from data in (15). †Estimate from the pK_a of PPh_2Cy (15).

stabilize unusual structures for Au(I) complexes (7, 10, 11). The distances between the Au atoms bonded to opposite ends of the N_2 unit are greater than 3.6 Å and are not bonding interactions.

Complexes **1** can be reduced to obtain NH_3 or mixtures of NH_3 and hydrazine. Treatment of tetrahydrofuran solutions of **1** with 20 equivalents of the proton source 2,6-lutidinium triflate ($2,6-Me_2C_5H_3N \cdot HO_3SCF_3$) and 10 equivalents of cobaltocene (Cp_2Co , a convenient organometallic reducing agent soluble in hydrocarbon solvents) produces NH_3 or NH_3 and hydrazine in combined yields of about 100% (12)



The yield of NH_3 , determined by the method of Chaney (13) using the procedures of Schrock *et al.* (14), and the yield of hydrazine, determined by the method of Watt and Chrisp (15), are inversely related and vary according to the phosphine ligand (Table 1) (16). Changes in either the basicity or the cone angle of the phosphine lead to variations in the NH_3 and hydrazine yields. The phosphine cone angle is constant whereas the basicity increases in the series PPh_3 , $P(p-MeC_6H_5)_3$, and $P(p-MeOC_6H_5)_3$. The observed increasing yields of NH_3 and the decreasing yields of hydrazine in this series suggest that the more basic phosphines promote NH_3 formation over hydrazine formation. However, $P(p-CF_3OC_6H_5)_3$ has the same cone angle but a lower basicity, yet the NH_3 yield with this phosphine is high. Determining the factors involved in the product distribution will require further investigation.

The Au products from the reduction reactions have not been characterized, except in the case of PPh_3 , where the known cluster $[(Ph_3PAu)_6]^{2+}$ (**2**) (2, 17) is the major Au-containing product. In principle, a catalytic cycle would be possible if cluster

2 would react with N_2 to form **1**. However, cluster **2** does not react with N_2 under any conditions so far employed. The reverse reaction, thermal decomposition of **1** to **2** and N_2 also does not occur (solid samples of **1** are stable to at least 140°C) (Fig. 3), suggesting that there is a kinetic barrier separating the N_2 complex **1** from cluster **2** and N_2 .

Complexes **1** are unique examples of N_2 bonded to six metal atoms. Recent results on the nitrogenase enzyme system have revealed the structure of the FeMo cofactor cluster where N_2 is bound and reduced (18). One proposal for the bonding of N_2 to this cluster involves entry of N_2 into the center of the cluster and bonding to six Fe atoms (18, 19) in a manner similar to the N_2 bonding of **1**.

REFERENCES AND NOTES

- For a recent review, see M. Hidai and Y. Mizobe, *Chem. Rev.* **95**, 1115 (1995).
- V. Ramamoorthy, Z. Wu, Y. Yi, P. R. Sharp, *J. Am. Chem. Soc.* **114**, 1526 (1992).
- A. V. Nesmeyanov *et al.*, *J. Organomet. Chem.* **201**, 343 (1980); Y. Yang and P. R. Sharp, *Inorg. Chem.* **32**, 1946 (1993); A. Kolb, P. Bissinger, H. Schmidbaur, *Z. Anorg. Allg. Chem.* **619**, 1580 (1993).
- Spectroscopic and analytical information is available from the corresponding author or to Science Online subscribers at <http://www.sciencemag.org/>
- Crystal data for **1** with L = PPh_2Pr (BF_4^- salt): from CH_2Cl_2/Et_2O , triclinic, space group $P-1$, unit cell dimensions $a = 12.2986(6)$ Å, $b = 14.4874(7)$ Å, $c = 14.6849(7)$ Å, $\alpha = 63.9440(10)^\circ$, $\beta = 86.7480(10)^\circ$, and $\gamma = 84.8350(10)^\circ$, unit cell volume $V = 2340.6(2)$ Å³, calculated crystal density = 1.953 g cm⁻³, number of formula units in unit cell $Z = 1$, absorption coefficient $\mu(MoK\alpha) = 9.529$ mm⁻¹, temperature $T = 293(2)$ K, 22,343 reflections measured, 10,028 unique after averaging, 7848 observed [$F > 4\sigma(F)$], 514 refined parameters, full-matrix least-squares refinement gave $R(F_{obs}) = 0.0484$, weighted $wR_2(F^2) = 0.1260$. Crystallographic details may be obtained from the corresponding author or from the Cambridge Crystallographic Data Centre, by quoting the full literature citation.
- E. W. Schmidt, *Hydrazine and its Derivatives* (Wiley, New York, 1984).
- H. Schmidbaur, *Gold Bull.* **23**, 11 (1990).
- P. Pyykkö and J. P. Desclaux, *Acc. Chem. Res.* **12**, 276 (1979).

9. H. Schmidbaur, W. Graf, G. Müller, *Angew. Chem. Int. Ed. Engl.* **27**, 417 (1988); M. Jansen, *ibid.* **26**, 1098 (1987); D. E. Harwell, M. D. Mortimer, C. B. Knobler, F. A. L. Anet, M. F. Hawthorne, *J. Am. Chem. Soc.* **118**, 2679 (1996).
10. P. G. Jones, *Gold Bull.* **14**, 102 (1981); *ibid.*, p. 159; *ibid.* **16**, 114 (1983); *ibid.* **19**, 46 (1986).
11. H. Schmidbaur, S. Hofreiter, M. Paul, *Nature* **377**, 503 (1995).
12. Mixtures of Cp_2Co and 2,6-lutidinium chloride have been used for catalytic reductions of hydrazine [K. D. Demadis, S. M. Malinak, D. Coucouvanis, *Inorg. Chem.* **35**, 4038 (1996)].
13. A. L. Chaney, *Clin. Chem.* **8**, 130 (1962).
14. R. R. Schrock, T. E. Glassman, M. G. Vale, M. Kol, *J. Am. Chem. Soc.* **115**, 1760 (1993).
15. G. W. Watt and J. D. Chrisp, *Anal. Chem.* **24**, 2006 (1952).
16. Md. Matiur Rahman, H.-Y. Liu, K. Eriks, A. Prock, W. Giering, *Organometallics* **8**, 1 (1989).
17. C. E. Briant, K. P. Hall, D. M. P. Mingos, *J. Organomet. Chem.* **229**, C5 (1982).
18. D. C. Rees, M. K. Chan, J. Kim, *Adv. Inorg. Chem.* **40**, 89 (1993); J. Kim and D. C. Rees, *Science* **257**, 1677 (1992); *Nature* **350**, 553 (1992); M. K. Chan, J. Kim, D. C. Rees, *Science* **260**, 792 (1993).
19. Early calculations disfavored internal bonding [H. Deng and R. Hoffmann, *Angew. Chem. Int. Ed. Engl.* **32**, 1062 (1993)]; however, more recent calculations are favorable [K. K. Stavrev and M. C. Zerner, *Chem. Eur. J.* **2**, 83 (1996)].
20. We thank J. Bercau for pointing out the structural analogy of **1** to the nitrogenase cluster. This work was supported by the Division of Chemical Sciences, Office of Basic Energy Sciences, Office of Energy Research, U.S. Department of Energy.

5 November 1996; accepted 3 January 1997

Optical Computation with Negative Light Intensity with a Plastic Bacteriorhodopsin Film

Aaron Lewis,* Yehuda Albeck, Zvi Lange, Julia Benchowski, Gavriel Weizman

The inability to use light intensity to represent negative values limits the potential of optical computing. The protein bacteriorhodopsin, an optically switchable bistable material, was used to represent an image as a local concentration of one of its two states. Light of one wavelength increased this concentration and represented positive intensity, whereas light of a different wavelength decreased the concentration and represented negative intensity. Optical subtraction was demonstrated by performing the mathematical operation of a difference of Gaussians. The electro-optical characteristics of bacteriorhodopsin films portend a variety of practical applications for this system.

Measurements of light intensity traditionally have allowed the recording of only positive values. Nonetheless, for practically every mathematical operation the representation of negative values is essential. Thus, the use of optical devices in computational schemes and image processing would be enhanced by the ability to directly find decreases in light intensity. For example, every optical device blurs the image of a single point; this spread of intensity limits the ability to resolve two closely spaced points of light. Although it is possible to reconstruct the real image mathematically, the required operations involve both positive and negative values. Here, we report how a bacteriorhodopsin (bR) film can be used to subtract two positive light intensities in order to represent a negative value.

We have prepared plastic bR films with high optical quality (1). The purple initial state of bR can be transformed into a relatively stable yellow form called M by absorption of a photon of the appropriate wavelength (2). This M state, in turn, can be switched back to the bR state by absorption of a photon of another wavelength. These light-driven state changes are more fully described in terms of the photocycle of bR (Fig. 1).

The value of a pixel in an image can be represented by the concentration of the bR or M state. Shining yellow light on a pixel would increase the concentration of the M state, whereas shining blue light would increase the concentration of the bR state. If a film is originally prepared with equal concentrations of bR and M, then negative and positive values can be represented as increases in the concentrations of bR or M that correspond to a surplus of blue or yellow light, respectively. We used this characteristic of such a bR film to approximate the operation of a difference of Gaussians

(DOG). This operation has historical importance as a method of edge enhancement in image processing (3).

Edge enhancement can be formulated as a map of loci where the Laplacian of the convolution of the image with a Gaussian changes sign (3). Thus, the edges of an image $I(x,y)$ are defined as the zero-crossing of the operator

$$\nabla^2 G(x,y) * I(x,y) = \nabla^2 \iint G(x-x',y-y') dx' dy' \quad (1)$$

where

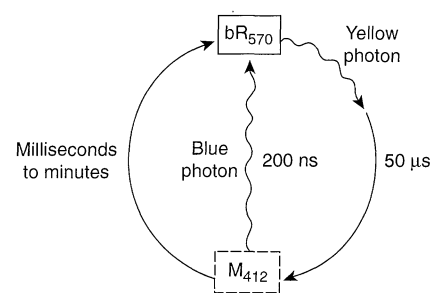
$$G(x,y) = \frac{1}{2\pi\sigma^2} \exp\left[-\left(\frac{x^2+y^2}{2}\right)\right] \quad (2)$$

Mathematically, however, $\nabla^2\{G * I\} = \{\nabla^2 G\} * I$. Thus, instead of convolving with a Gaussian and then taking the Laplacian, it is possible to convolve with the Laplacian of a Gaussian. Moreover, the Laplacian of the Gaussian can be approximated by a DOG. Explicitly, this DOG can be written as

$$\nabla^2 G(x,y,\sigma) = G(x,y,\sigma_1) - G(x,y,\sigma_2) \quad (3)$$

where σ_1 and σ_2 are the widths of two two-dimensional Gaussians. These widths should have a ratio of 1:1.6 if the DOG is to approximate $\nabla^2 G(x,y,\sigma)$ (4). An example of such an approximation for a one-dimen-

Fig. 1. The photoinduced cycle of bR with the two intermediates of importance for this study. The bR state absorbs a yellow photon within the broad bR absorption with a maximum at 570 nm. This transforms into intermediate states (not shown) and then decays to the relatively stable M state within 50 μ s. M is thermally transformed into the initial pigment bR; the lifetime of this transition depends on the sample preparation. The M state can be converted into the bR state within 200 ns by absorption of a blue photon (2). Stable, optically uniform films of bR can be produced by embedding bR in a polyvinyl alcohol (PVA) polymer matrix (1). These films can withstand normal environmental conditions over many years of operation. To obtain a good-contrast film, we mixed bR with PVA at a 1:5 ratio. The bR suspension had an initial optical density of ~ 19.2 , which resulted in a film with an optical density of ~ 4 . In this film the lifetime of the M state at room temperature was several minutes. This lifetime can be varied from a few milliseconds for wet samples to several hours in samples that are dried at high pH. However, in all of these samples, the yellow and purple light produce a photostationary concentration of bR and M in as fast as tens of microseconds. The absorption bands of M and bR do not overlap, so relatively low power is needed to switch a sample from one pure state to another.



Division of Applied Physics and Center for Neural Computation, Hebrew University of Jerusalem, Jerusalem 91904, Israel.

* To whom correspondence should be addressed. E-mail: lewisu@vms.huji.ac.il